Published in final edited form as:
J Hepatol. 2007 August ; 47(2): 262–269.

SUCCINATE IS A PARACRINE SIGNAL FOR LIVER DAMAGE

Paulo Renato A. V. Correa[1], **Emma A. Kruglov**[1], **Mayerson Thompson**[1,2], **M. Fatima Leite**[2], **Jonathan A. Dranoff**[1], and **Michael H. Nathanson**[1,3]

1*Section of Digestive Diseases, Department of Internal Medicine, Yale University School of Medicine, New Haven, CT 06520-8019 USA*

2*Department of Physiology and Biophysics, Federal University of Minas Gerais, Belo Horizonte, MG 31270-901, Brazil*

SUMMARY

Background and Aims: A G-protein coupled succinate receptor has recently been identified in several tissues, including the liver. The objectives of this work were to determine the hepatic cell types that express this receptor and to determine its physiological role.

Methods: Expression and distribution of the succinate receptor was determined by RT-PCR and confocal immunofluorescence. Biochemical assays were used to measure succinate and cAMP. Cytosolic Ca^{2+} was monitored in single cells by time-lapse imaging. Western blot was used to study the effect of succinate on activation of hepatic stellate cells.

Results: The succinate receptor was expressed in quiescent hepatic stellate cells, and expression decreased with activation. Ischemia induced release of succinate in isolated perfused livers. In contrast to what is observed in cell expression systems, succinate did not inhibit cAMP production or increase cytosolic Ca^{2+} in primary hepatic stellate cells. However, succinate accelerated stellate cell activation.

Conclusions: Hepatic stellate cells express the succinate receptor. Succinate may behave as a paracrine signal by which ischemic hepatocytes trigger stellate cell activation.

Keywords

GPR91; succinate receptor; stellate cells; liver; ischemia; signal transduction

INTRODUCTION

Succinate is an important metabolic molecule that constitutes one of the intermediates of the citric acid cycle. Recently, a succinate receptor was identified that suggests succinate may also act a signaling molecule (1). This newly described receptor is the former orphan G-protein-coupled receptor GPR91. This receptor is expressed in kidney, liver, spleen and to a lesser extent small intestine (1). The distribution and function of the succinate receptor within the kidney has been examined, but nothing is known about the receptor in the liver. The principal signaling actions of succinate that are mediated by the receptor GPR91 in kidney are to increase Ca^{2+} via Gq and to decrease cAMP via Gi. The principal downstream effect that has been identified is an increase in renin release, which produces a rise in arterial blood pressure (1).

[3]**Address for correspondence:** Michael H. Nathanson Digestive Diseases, Room TAC S241D Yale University School of Medicine New Haven, CT 06520-8019 USA Phone 203-785-7312, FAX 203-785-4306 Email: michael.nathanson@yale.edu

Given the important role of succinate as an intermediary of the central cross-road of metabolism – the citric acid cycle – and its novel signaling properties, an attractive hypothesis is that GPR91 might serve as a sensor of metabolic activity in organs or tissues. Of special interest is the fact that succinate levels rise in response to ischemia (2;3), because GPR91 could be responsible for mediating the adaptation of organs and tissues to hypoxic conditions, including regulating secretion or repair and proliferation. Because the liver is the central metabolic organ and is particularly susceptible to ischemia, we examined the intrahepatic distribution and functional role of the succinate receptor.

MATERIAL AND METHODS

Animals and materials

Male Sprague-Dawley rats (200-250 g, Charles River Laboratories, Boston, MA) were used for all studies. Animals were maintained on a standard diet and housed under a 12-hour light-dark cycle. Ultra-pure succinic acid and ATP were purchased from Sigma Chemical Co. (St. Louis, MO). All other chemicals were of the highest quality commercially available.

Isolation of hepatic cell types

Hepatic stellate cells (HSC) were isolated from male Sprague Dawley rats by Nycodenz gradient centrifugation, as described previously (4). Primary cells were >95% pure. Cells were grown on glass coverslips in DMEM-F12 medium with 10% FCS. At day 1 after isolation HSC are phenotypically quiescent, while by day 7 they have become phenotypically activated. Portal fibroblasts were isolated from biliary trees as described previously (5), following *in situ* pronase/collagenase perfusion of male Sprague Dawley rat livers. The biliary tree was minced and digested by collagenase, pronase and deoxyribonuclease, then filtered through 30 μm nylon mesh. The resulting cells were grown on tissue culture flasks in DMEM-F12 medium with 10% FCS. Hepatocytes and cholagiocytes were isolated by collagenase perfusion, according to protocols described previously (6;7). Kupffer cells were isolated by collagenase perfusion followed by centrifugal elutriation (8) and their purity was confirmed by immunostaining with commercially obtained antibodies (Serotec; Dusseldorf, Germany) for the Kupffer cell marker F4/80 (9), while sinusoidal endothelial cells were isolated by collagenase perfusion followed by Percoll gradient centrifugation (10) and their purity was confirmed by staining with commercially obtained antibodies for endothelial nitric oxide synthase (eNOS) (BD Biosciences; San Jose, CA).

RT-PCR for GPR91

RNA was isolated from various tissues and cells using RNAqueous (Ambion, Austin, TX). RNA obtained from whole liver, hepatocytes, cholangiocytes, quiescent and activated hepatic stellate cells, quiescent and activated portal fibroblasts and kidney were reversely transcribed into cDNA by using SuperScript First-Strand Synthesis System for RT-PCR (Invitrogen, La Jolla, CA) according to the manufacturer's instruction. The resulting cDNA was amplified by PCR using 45 μL of PCR SuperMix (Invitrogen, La Jolla, CA) and 250nM of both sense and antisense primers for rat GPR91. The samples were subjected to 30 cycles consisting of: 30 sec. at 94°C, 30 sec. at 58°C and 1 min. at 72°C. This was followed by a final extension at 72° C for 10 min. The primers were designed using the software Primer3 (11) based on the sequence deposited in the NCBI Nucleotide Bank (AY612851). The forward primer sequence was 5′ -TTACGCCACTGGGAACTGGA-3′ and the reverse primer sequence 5′ -TTGATGGCCTTCTGGGAACA-3′ . The primers for the GAPDH were designed based on the Rattus norvegicus sequence deposited in the NCBI nucleotide bank (NM_017008). The forward primer sequence was 5'-TGCCACTCAGAAGACTGTGG-3' and the reverse primer sequence 5'-TTCAGCTCTGGGATGACCTT-3'. The PCR program for GAPDH consisted of 25 cycles of: 30 sec. at 94°C, 30 sec. at 60°C and 1 min. at 72°C, followed by a final extension

at 72°C for 10 min. Both PCR reactions were performed in a PTC-100 automated thermocycler and the expected PCR products of 641 bp and 128 bp for the GPR91 and GAPDH respectively were subjected to agarose gel electrophoresis in TAE buffer, stained with ethidium bromide and visualized using a UV-light transilluminator.

Immunofluorescence

Confocal immunofluorescence histochemistry was performed on 4-μm-thick frozen sections of rat liver as described previously (12). The frozen tissue sections were fixed and permeabilized by cold acetone. After blocking steps, specimens were labeled with primary antibodies for GPR91 (Chemicon International, Temecula, CA) and the stellate cell marker desmin (Sigma, S. Louis, MO), rinsed with phosphate-buffered saline, and incubated with fluorescent secondary antibodies (Invitrogen, Eugene, Oregon). Primary antibodies used were anti-desmin mouse monoclonal (1:50) and anti-GPR91 rabbit polyclonal (1:25). Secondary antibodies were Alexa 488 anti-rabbit (1:500) and Alexa 568 anti-mouse (1:500). Tissue also was labeled with the actin stain Alexa 647-conjugated phalloidin (Invitrogen) to facilitate identification of individual cells. For negative control studies, tissue was incubated with secondary antibodies, but primary antibodies were omitted. In single cell studies, freshly isolated stellate cells were double-labeled with GPR91 and a mouse monoclonal antibody directed against the quiescent stellate cell marker glial fibrillary acidic protein (GFAP, 1:100; Abcam; Cambridge, MA) (13). Specimens were examined with a Zeiss LSM 510 META Laser Scanning Confocal Microscope equipped with argon and helium/neon lasers (Thornwood, NY). To ensure specificity of staining, images were obtained by using confocal machine settings (i.e., aperture, gain, and black level) at which no fluorescence was detectable in negative control samples labeled with secondary antibodies alone. Immunofluorescence images were obtained by excitation at 488 nm with observation at 505–550 nm to detect Alexa 488, by excitation at 543 nm and observed at 560–615 nm to detect Alexa 568, then by excitation at 633 nm with observation at >650 nm to detect Alexa 647. This approach eliminated bleed-through of Alexa 488 fluorescence into the longer wavelength detection channel. These confocal images used a Plan Apochromat 63x, 1.20 numeric aperture water immersion objective, argon (488 nm) and helium/neon (543 and 633 nm) laser lines, and a confocal pinhole adjusted to obtain a 1-μm depth of focus.

Isolated perfused rat liver studies

Liver perfusions were performed as described previously (14). The pancreatoduodenal branch of the portal vein was ligated and the bile duct, portal vein and inferior vena cava were cannulated with the animal under pentobarbital anesthesia (50 mg/kg of body weight). The liver was transferred to a chamber maintained at 37°C and perfused at 40 ml/min with Krebs-Ringer bicarbonate (KRB) buffer containing 5 mM glucose and gassed with 95% O2/5% CO2. Using a single-pass system, bile flow was measured gravimetrically in pre-tared tubes and perfusion pressure was monitored continuously before, during and after isolated perfused rat livers (IPRLs) were infused with succinate (100μM). Viability of each IPRL was assessed by observing portal pressure and bile flow throughout each experiment. In addition, each liver was examined for evidence of mottling or other gross morphological changes, and trypan blue was added to the perfusate at the end of each experiment to assess the adequacy of vascular perfusion. Hepatic glucose release was measured throughout the course of experiments as an additional index of effects on hepatocytes.

Succinate assay

Succinate released from the liver was measured directly in IPRL effluent. The perfusion buffer was collected in plastic tubes after it passed through the liver and placed immediately on ice. The concentration of succinate in those samples was tested by using the Succinic Acid Assay

Procedure (Megazyme, Bray, Ireland), which applies the method of succinyl-CoA synthase, pyruvate kinase, and lactate dehydrogenase, according to Beutler (15). The principle of this method is that in the presence of adenosine-5'-triphosphate (ATP), succinate is converted to succinyl-CoA by the enzyme succinyl-CoA synthetase (SCS), with the concurrent formation of adenosine-5'-diphosphate (ADP) and inorganic phosphate (Pi). In the presence of pyruvate kinase, ADP reacts with phosphoenolpyruvate (PEP) to form pyruvate and ATP. The pyruvate produced is reduced to L-lactate by L-lactate dehydrogenase (L-LDH) in the presence of reduced nicotinamideadenine dinucleotide (NADH), with the production of NAD^+. The amount of NAD^+ formed in the above coupled reaction pathway is stoichiometric with the amount of succinate. The consumption of NADH, that corresponds to the NAD^+ formed, is measured by the decrease in absorbance at 340 nm and indicates the amount of succinate.

Cyclic AMP Measurements

The production of cAMP was measured using the cAMP Biotrak Enzymeimmunoassay (EIA) System (Amersham Biosciences, Piscataway, NJ). Cells were cultured overnight on 96-well tissue culture plates at a density of 10^5 cells/ml and stimulated with succinate (1 mM), forskolin (10 μM) or both, for 10 minutes at 37°C. The assay was performed according to the manufacturer's instructions and absorbance was read at 450 nm. The concentration of cAMP per well was obtained by correlating absorbance of samples with absorbance obtained standard curve.

Cytosolic Ca^{2+} measurements

Ca^{2+} measurements were performed on hepatic stellate cells (HSC) by time-lapse confocal microscopy (7;16). Cells were loaded with the Ca^{2+} dye fluo-4/AM (Molecular Probes-Invitrogen, Carlsbad, California). Coverslips containing the dye-loaded cells were transferred to a chamber on the stage of a Zeiss LSM 510 confocal microscope, and then perfused with a HEPES-buffered solution (in mM: NaCl, 130; KCl, 5; $CaCl_2$, 1.25; KH_2PO_4, 1.2; $MgSO_4$, 1; HEPES, 19.7; glucose, 5; pH 7.4). Ca^{2+} was monitored in these cells by exciting the specimen at 488 nm and detecting emission signals above 515 nm. A 15 mW krypton-argon laser was used for excitation. Optical sections 1 to 2 μm in thickness were obtained. Cells were observed with a 40x, 1.3 numeric aperture water objective. Increases in Ca^{2+} were expressed in terms of percentage increase in fluorescence intensity of fluo-4. Neither autofluorescence nor other background signals were detected at the machine settings used, and there was no change in size, shape or location of cells during experiment.

Immunoblots

Protein was extracted and subject to sodium-dodecyl-sulphate polyacrylamide gel electrophoresis (SDS-PAGE) in 4 – 20% Tris-HCl gradient gels. Gels were transferred to PVDF membranes followed by antibody labeling as described previously (17). Primary antibodies used were: mouse monoclonal anti-α-smooth muscle actin (Sigma-Aldrich) and mouse monoclonal anti-GAPDH (Ambion, Houston, TX). Secondary antibodies were goat anti-mouse IgG linked to horseradish peroxidase (HRP) (Amersham Biosciences, Piscataway, NJ) and rabbit anti-rat IgG HRP-linked (Stressgen, Victoria, BC). Westerns were developed with ECL plus reagent (Amersham Biosciences, Piscataway, NJ). Quantitative measurements were made by scanning the films with a GS-700 imaging densitometer (BioRad) and then analyzing these images using ImageJ software (NIH, Bethesda, MD).

Statistics

Results are expressed as mean values ± S.D., except where otherwise noted. SigmaPlot (Systat Software, Point Richmond, CA) and Prism (GraphPad Software, San Diego, CA) were used

for data analysis. Statistical significance was tested using Student's *t* test and a p value <0.05 was taken to indicate statistical significance.

RESULTS

Expression and distribution of the succinate receptor in liver

Expression of the succinate receptor GPR91 was detected in rat liver using RT-PCR of mRNA extracted from whole liver samples (Figure 1). The tissue distribution of this receptor was characterized by isolating hepatocytes, cholangiocytes, Kupffer cells, sinusoidal endothelial cells, hepatic stellate cells and portal fibroblasts and the mRNA specific for each of these cell types was extracted. The succinate receptor GPR91 was detected only in quiescent hepatic stellate cells (HSC), as well as in whole liver and kidney positive controls (Figure 1a). The expression of the succinate receptor was lost in activated HSC, as determined in samples from cells seven days in culture after isolation (Figure 1a), as well as in stellate cells that had been passaged three times (Figure 1b). Message for the succinate receptor was not detected in hepatocytes, cholangiocytes, or portal fibroblasts (Figure 1a). Message also was not detected in Kupffer cells or sinusoidal endothelial cells (Figure 1b). These findings suggest the expression of the succinate receptor GPR91 by hepatic stellate cells accounts for the principal expression observed in whole liver samples. The cellular distribution of the succinate receptor was also examined by confocal immunofluorescence in rat liver and in isolated stellate cells (Figure 2). Staining for GPR91 co-localized with labeling for the HSC markers desmin (Figures 2a-b) and GFAP (Figure 2c). These findings confirm that, in the liver, the succinate receptor is expressed primarily in hepatic stellate cells.

Succinate and the perfused liver

Succinate (100 μM) infusion via the portal vein had no effect on perfusion pressure, which remained nearly constant during succinate infusion (Figure 3a). Glucose output was also unaffected by succinate infusion (Figure 3b). These findings suggest that succinate plays a minimal role in these particular physiological functions, consistent with its lack of expression in hepatocytes and cholangiocytes. However, hepatocytes are the principal source of succinate in the liver, so we examined whether ischemia induces succinate release. To induce ischemia, portal flow was interrupted for 30 min. Ischemia grossly was reflected by the mottled appearance of the liver at the end of the experiment, as compared to a normal appearance in control experiments. The succinate level in the perfusate effluent rose 14-fold, as compared to baseline, after ischemia was produced by stopping buffer flow (Figure 3c). The concentrations of succinate detected reached more than 1 mM, almost 20 times the EC_{50} of 56±8 μM calculated for the binding of succinate to its receptor GPR91. Therefore, hepatic ischemia is accompanied by intense release of succinate.

Effect of succinate on signaling pathways

The cloned GPR91 receptor activates Gi and Gq when expressed in HEK-293 cells (1), so we examined whether either of these G proteins are activated in quiescent HSC exposed to succinate. Succinate had no effect on cAMP production in HSC (Figure 4). In addition, it did not inhibit the production of cAMP induced by forskolin (10μM) (Figure 4). These findings suggest that GPR91 does not couple to Gi in quiescent HSC. Similarly, succinate in concentrations up to 1 mM did not increased cytosolic Ca^{2+} in quiescent HSC (Figure 5). The cells that did not respond to succinate were then stimulated with ATP (100μM), since HSC express P2Y receptors that link to Ca^{2+} signaling via Gq (4). In each cell, ATP induced a rapid increase in Ca^{2+}. These findings suggest that the succinate receptor does not link to Gq in HSC.

Effect of succinate on hepatic stellate cell activation

Stellate cells undergo myofibroblastic transdifferentiation (commonly denoted “activation”) in liver injury. Upregulation of alpha-smooth muscle actin (α-SMA), a hallmark of myofibroblastic transdifferentiation, was used as a marker for HSC activation (18). α-SMA was not detected in HSC one day after isolation, and was maximal by 5 days after isolation (Figure 6). α-SMA expression in control HSC reached 29% of maximum 3 days after isolation, but was over twice this amount in HSC treated with 400 μM succinate ($p<0.05$). The maximum amount of α-SMA detected in activated HSC 5 days after isolation was similar in control and succinate-treated cells. These findings suggest that succinate accelerates activation of hepatic stellate cells.

DISCUSSION

Succinate is an intermediary of the citric acid cycle, a central metabolic pathway which promotes the oxidative decarboxylation of acetyl-CoA and produces reducing equivalents, NADH and $FADH_2$, used in the respiratory chain (2). Succinate is produced by the oxidation of succinyl-CoA by the enzyme succinyl-CoA hydrolase and is further oxidized to fumarate by succinate dehydrogenase. The activity of the citric acid cycle is regulated to match metabolic demands (2), but pathological situations such as ischemia can disrupt the flow of substrates in this cycle (19), resulting in increased succinate levels (2;3).

A G-protein coupled receptor for succinate was described which has sequence homology with the P2Y1 purinergic receptor (1). The calculated EC_{50} was 56 μM and the receptor was specific for succinate rather than other citric acid cycle intermediates. In cell expression systems, it coupled through Gi and Gq to inhibit adenylate cyclase and increase cytosolic Ca^{2+}, respectively. The succinate receptor is primarily expressed in kidney, followed by liver, spleen and small intestine. In kidney it is expressed in the renal cortex, predominantly in the proximal tubules, and to a lesser extent in the distal tubules. The renal succinate receptor has been localized only by *in situ* hybridization (1), so it is not known which renal cell types express it. Intravenous injections of succinate in rats increased plasma renin activity and caused a dose-dependent increase in mean arterial pressure, and nephrectomy abolished this effect. Captopril, an inhibitor of the reninangiotensin system, attenuated the hypertensive effect of succinate. Succinate receptor knockout mice have no discernable phenotype, but succinate does not induce hypertension in these animals. However, angiotensin II increases blood pressure to a similar extent in wild-type and succinate receptor-deficient mice. The hypertensive effect of succinate is mediated by the succinate receptor through the activation of the renin–angiotensin system. The molecular mechanism of renin release by succinate remains unexplained, because the succinate receptor appears to couple through Gi and Gq, while renin release is usually triggered by Gs activation. Our finding that succinate does not increase hepatic perfusion pressure suggests that actions of succinate in the liver do not contribute to the hypertensive effects of this metabolite.

Hepatic stellate cells react to a range of signals to respond to liver injury. A number of growth factors and hormones can induce stellate cell activation, including transforming growth factor-β, platelet-derived growth factor, and endothelin-1 (18;20). Increased stiffness of the extracellular matrix also leads to stellate cell activation (21;22), and the combination of mechanical tension and TGF-β stimulation may be a particularly effective combination (23). Hepatic necrosis activates stellate cells in part through reactive oxygen intermediates and initiation of oxidant stress-related pathways (20;24), whereas apoptotic hepatocytes activate stellate cells via released apoptotic fragments (25) as well as Fas-related pathways (26). HSC also can react to signals induced by bile acids, both via plasma membrane receptors (27) and via nuclear hormone receptors (28). Thus, stellate cells can be regulated by both traditional signals such as growth factors and hormones, and by nontraditional signals such as matrix

stiffness, oxidant stress, and metabolites. The current work extends our understanding of how liver damage can activate stellate cells by showing that stellate cells can detect not only lethal hepatocyte damage but sublethal damage as well. To this end, the current findings indicate that succinate behaves as a metabolic sensor in the liver. Succinate is produced and consumed in the central pathway of metabolism, and its levels are altered by changes in tissue metabolic activity and insults, while the succinate receptor acts to transduce the resulting concentrations of extracellular succinate into intracellular signals in stellate cells.

What are the signaling pathways activated by the succinate receptor in stellate cells? Although the receptor activates Gq and Gi in the CHO and HEK-293 cell lines (1), our findings suggest that it does not activate these G proteins in stellate cells. Indeed, specific G protein-coupled receptors can promiscuously couple to and activate multiple G proteins (29;30), and downstream effects of receptor activation depend on which G proteins are activated (31). Therefore, our findings may reflect differences in expression levels of the endogenous succinate receptor or of its possible G protein partners in stellate cells, relative to transfected CHO or HEK-293 cells. Our findings also do not rule out the possibility that stimulation of the succinate receptor potentiates the effects of other factors that are known to induce stellate cell activation, as discussed above. Finally, although we found that Kupffer cells do not express the succinate receptor, anti-oxidant properties of succinate have been shown to affect gene expression and cytokine release in these cells (32), suggesting an even more complex interaction among the various hepatic cell types in response to ischemia. Further work will be needed to understand the relative importance of this novel pathway in the response to liver damage, and to define the mechanisms by which the succinate receptor links to stellate cell activation pathways.

ACKNOWLEDGEMENTS

This work was supported by NIH grants DK45710, DK34989 and TW01451.

REFERENCES

1. He W, Miao FJ, Lin DC, Schwandner RT, Wang Z, Gao J, Chen JL, Tian H, Ling L. Citric acid cycle intermediates as ligands for orphan G-protein-coupled receptors. Nature 2004;429:188–93. [PubMed: 15141213]
2. Krebs HA. Rate control of the tricarboxylic acid cycle. Adv Enzyme Regul 1970;8:335–53. [PubMed: 4920378]
3. Hems DA, Brosnan JT. Effects of ischaemia on content of metabolites in rat liver and kidney in vivo. Biochem J 1970;120:105–11. [PubMed: 4321927]
4. Dranoff JA, Ogawa M, Kruglov EA, Gaca MD, Sevigny J, Robson SC, Wells RG. Expression of P2Y nucleotide receptors and ectonucleotidases in quiescent and activated rat hepatic stellate cells. Am J Physiol Gastrointest Liver Physiol 2004;287:G417–G424. [PubMed: 14764443]
5. Jhandier MN, Kruglov EA, Lavoie EG, Sevigny J, Dranoff JA. Portal fibroblasts regulate the proliferation of bile duct epithelia via expression of NTPDase2. J Biol Chem 2005;280:22986–92. [PubMed: 15799977]
6. Hirata K, Pusl T, O'Neill AF, Dranoff JA, Nathanson MH. The type II inositol 1,4,5-trisphosphate receptor can trigger Ca2+ waves in rat hepatocytes. Gastroenterology 2002;122:1088–100. [PubMed: 11910359]
7. Schlosser SF, Burgstahler AD, Nathanson MH. Isolated rat hepatocytes can signal to other hepatocytes and bile duct cells by release of nucleotides. Proc Natl Acad Sci U S A 1996;93:9948–53. [PubMed: 8790437]
8. Holstege A, Leser HG, Pausch J, Gerok W. Uridine catabolism in Kupffer cells, endothelial cells, and hepatocytes. Eur J Biochem 1985;149:169–73. [PubMed: 3922756]

9. Kato T, Takeya M, Takagi K, Takahashi K. Chemically induced transplantable malignant fibrous histiocytoma of the rat. Analyses with immunohistochemistry, immunoelectron microscopy and [3H] thymidine autoradiography. Lab Invest 1990;62:635–45. [PubMed: 2160564]
10. De Leeuw AM, Barelds RJ, de Zanger R, Knook DL. Primary cultures of endothelial cells of the rat liver: a model for ultrastructural and functional studies. Cell Tissue Res 1982;223:201–15. [PubMed: 7066967]
11. Rozen S, Skaletsky H. Primer3 on the WWW for general users and for biologist programmers. Methods Mol Biol 2000;132:365–86. [PubMed: 10547847]
12. Hirata K, Pusl T, O'Neill AF, Dranoff JA, Nathanson MH. The type II inositol 1,4,5-trisphosphate receptor can trigger Ca2+ waves in rat hepatocytes. Gastroenterology 2002;122:1088–100. [PubMed: 11910359]
13. Neubauer K, Knittel T, Aurisch S, Fellmer P, Ramadori G. Glial fibrillary acidic protein--a cell type specific marker for Ito cells in vivo and in vitro. J Hepatol 1996;24:719–30. [PubMed: 8835748]
14. Hirata K, Nathanson MH. Bile duct epithelia regulate biliary bicarbonate excretion in normal rat liver. Gastroenterology 2001;121:396–406. [PubMed: 11487549]
15. Beutler, HO. Succinate. In: Bergmeyer, HU., editor. Methods of Enzymatic Analysis. VCH Publishers (UK) Ltd.; Cambridge, UK: 1989. p. 25-33.
16. Shibao K, Hirata K, Robert ME, Nathanson MH. Loss of inositol 1,4,5-trisphosphate receptors from bile duct epithelia is a common event in cholestasis. Gastroenterology 2003;125:1175–87. [PubMed: 14517800]
17. Hirata K, Pusl T, O'Neill AF, Dranoff JA, Nathanson MH. The type II inositol 1,4,5-trisphosphate receptor can trigger Ca2+ waves in rat hepatocytes. Gastroenterology 2002;122:1088–100. [PubMed: 11910359]
18. Knittel T, Janneck T, Muller L, Fellmer P, Ramadori G. Transforming growth factor beta 1-regulated gene expression of Ito cells. Hepatology 1996;24:352–60. [PubMed: 8690404]
19. Peuhkurinen KJ, Takala TE, Nuutinen EM, Hassinen IE. Tricarboxylic acid cycle metabolites during ischemia in isolated perfused rat heart. Am J Physiol 1983;244:H281–H288. [PubMed: 6824095]
20. Friedman SL. Molecular regulation of hepatic fibrosis, an integrated cellular response to tissue injury. J Biol Chem 2000;275:2247–50. [PubMed: 10644669]
21. Friedman SL, Roll FJ, Boyles J, Arenson DM, Bissell DM. Maintenance of differentiated phenotype of cultured rat hepatic lipocytes by basement membrane matrix. J Biol Chem 1989;264:10756–62. [PubMed: 2732246]
22. Sohara N, Znoyko I, Levy MT, Trojanowska M, Reuben A. Reversal of activation of human myofibroblast-like cells by culture on a basement membrane-like substrate. J Hepatol 2002;37:214–21. [PubMed: 12127426]
23. Wells RG. The role of matrix stiffness in hepatic stellate cell activation and liver fibrosis. J Clin Gastroenterol 2005;39:S158–S161. [PubMed: 15758652]
24. Friedman SL. Mechanisms of disease: Mechanisms of hepatic fibrosis and therapeutic implications. Nat Clin Pract Gastroenterol Hepatol 2004;1:98–105. [PubMed: 16265071]
25. Canbay A, Taimr P, Torok N, Higuchi H, Friedman S, Gores GJ. Apoptotic body engulfment by a human stellate cell line is profibrogenic. Lab Invest 2003;83:655–63. [PubMed: 12746475]
26. Canbay A, Higuchi H, Bronk SF, Taniai M, Sebo TJ, Gores GJ. Fas enhances fibrogenesis in the bile duct ligated mouse: a link between apoptosis and fibrosis. Gastroenterology 2002;123:1323–30. [PubMed: 12360492]
27. Brady LM, Beno DW, Davis BH. Bile acid stimulation of early growth response gene and mitogen-activated protein kinase is protein kinase C-dependent. Biochem J 1996;316(Pt 3):765–9. [PubMed: 8670150]
28. Fiorucci S, Antonelli E, Rizzo G, Renga B, Mencarelli A, Riccardi L, Orlandi S, Pellicciari R, Morelli A. The nuclear receptor SHP mediates inhibition of hepatic stellate cells by FXR and protects against liver fibrosis. Gastroenterology 2004;127:1497–512. [PubMed: 15521018]
29. Gudermann T, Kalkbrenner F, Schultz G. Diversity and selectivity of receptor-G protein interaction. Annu Rev Pharmacol Toxicol 1996;36:429–59. [PubMed: 8725397]

30. Kukkonen JP, Nasman J, Akerman KEO. Modelling of promiscuous receptor-G(i)/G(s) - protein coupling and effector response. Trends in Pharmacological Sciences 2001;22:616–22. [PubMed: 11730971]

31. Lechleiter J, Girard S, Clapham D, Peralta E. Subcellular Patterns of Calcium Release Determined by G-Protein-Specific Residues of Muscarinic Receptors. Nature 1991;350:505–8. [PubMed: 1849616]

32. Tsukamoto H, Rippe R, Niemela O, Lin M. Roles of Oxidative Stress in Activation of Kupffer and Ito Cells in Liver Fibrogenesis. Journal of Gastroenterology and Hepatology 1995;10:S50–S53. [PubMed: 8589343]

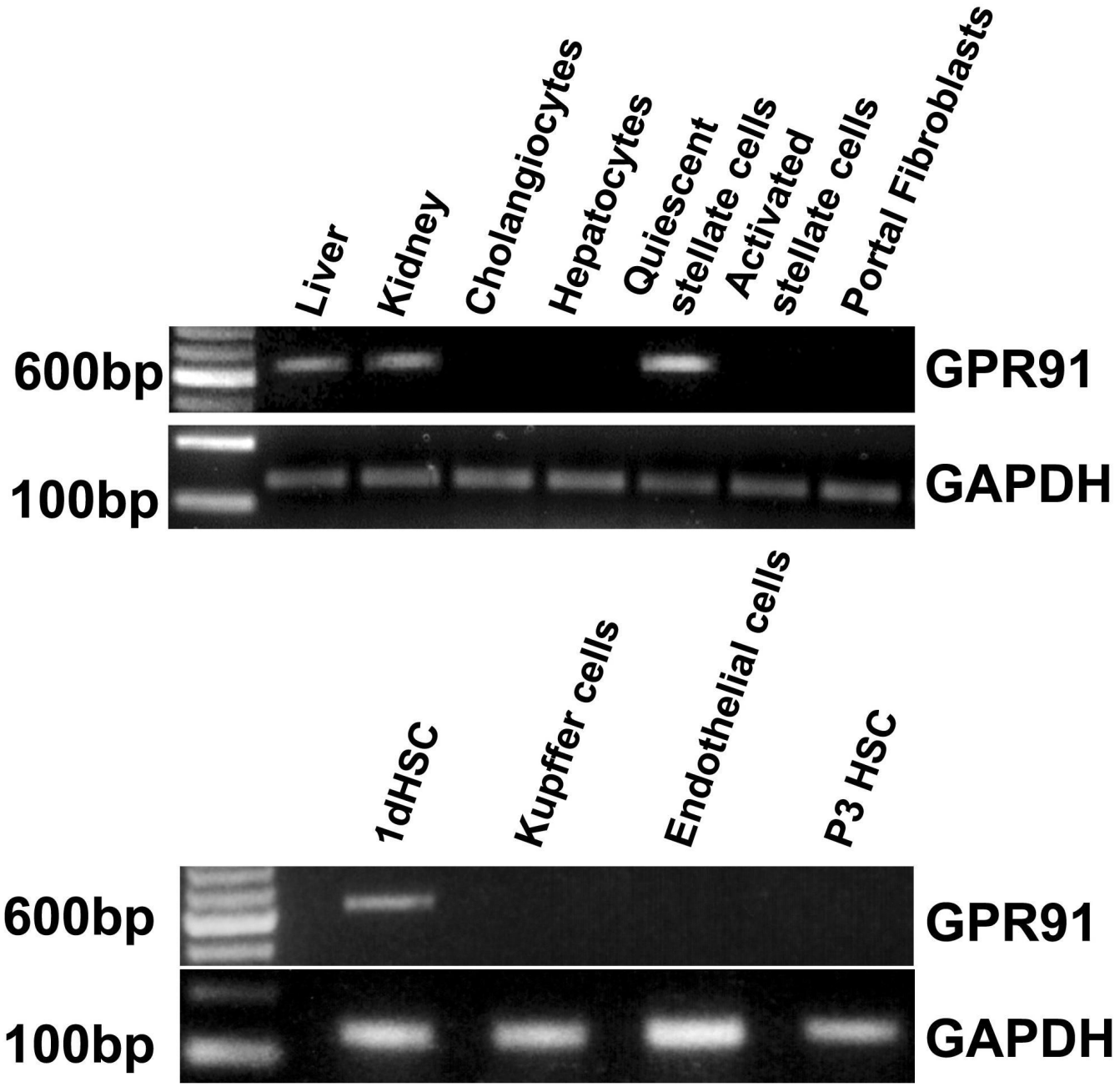

Figure 1.

The succinate receptor GPR91 is expressed in quiescent hepatic stellate cells. **(a)** The 641 base-pair PCR product is found in whole liver samples and hepatic stellate cells, but not in isolated hepatocytes, cholangiocytes, portal fibroblasts, or activated hepatic stellate cells. The positive control, kidney, shows the same product. **(b)** The PCR product found in quiescent hepatic stellate cells (1d HSC) is not in passaged stellate cells (P3 HSC) or in Kupffer cells or sinusoidal endothelial cells. PCR for GAPDH was used as a loading control in both gels.

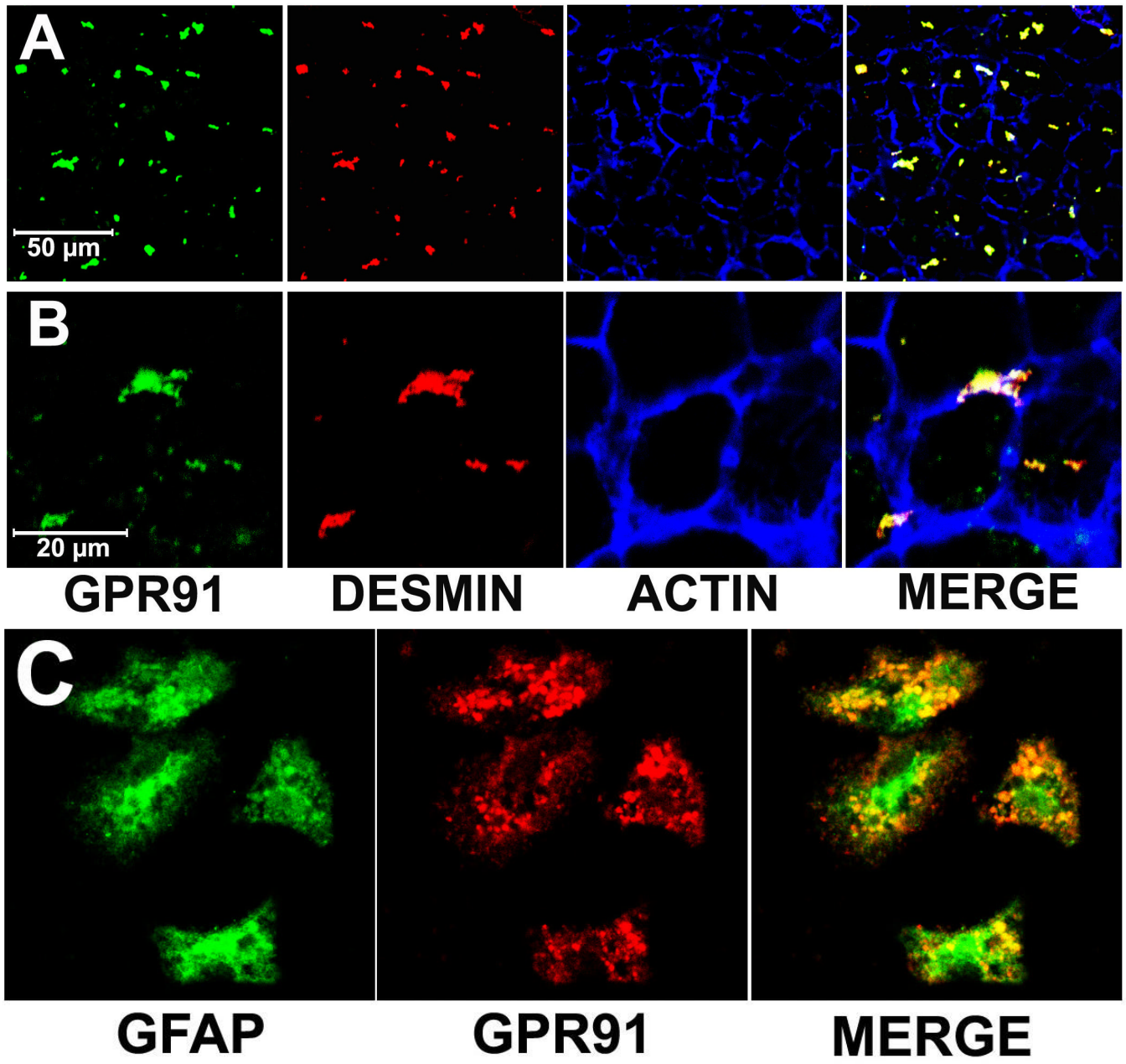

Figure 2.

Visualization of the succinate receptor in hepatic stellate cells. **(a)** Low-magnification and **(b)** high-magnification confocal immunofluorescence images of rat liver show that staining for the succinate receptor (green) and the HSC marker desmin (red) co-localize (yellow). The actin label phalloidin (blue) outlines individual hepatocytes for reference. No non-specific staining is seen in liver sections labeled with secondary antibody alone (not shown). **(c)** Confocal immunofluorescence image of isolated hepatic stellate cells after 24 hr in culture. The cells are stained for the quiescent stellate cell marker GFAP (green, left) and for the succinate receptor (red, center). Note on the merged image (right) that some of the succinate receptor staining is peripheral to GFAP staining. No non-specific staining is seen in stellate cells labeled with secondary antibody alone (not shown).

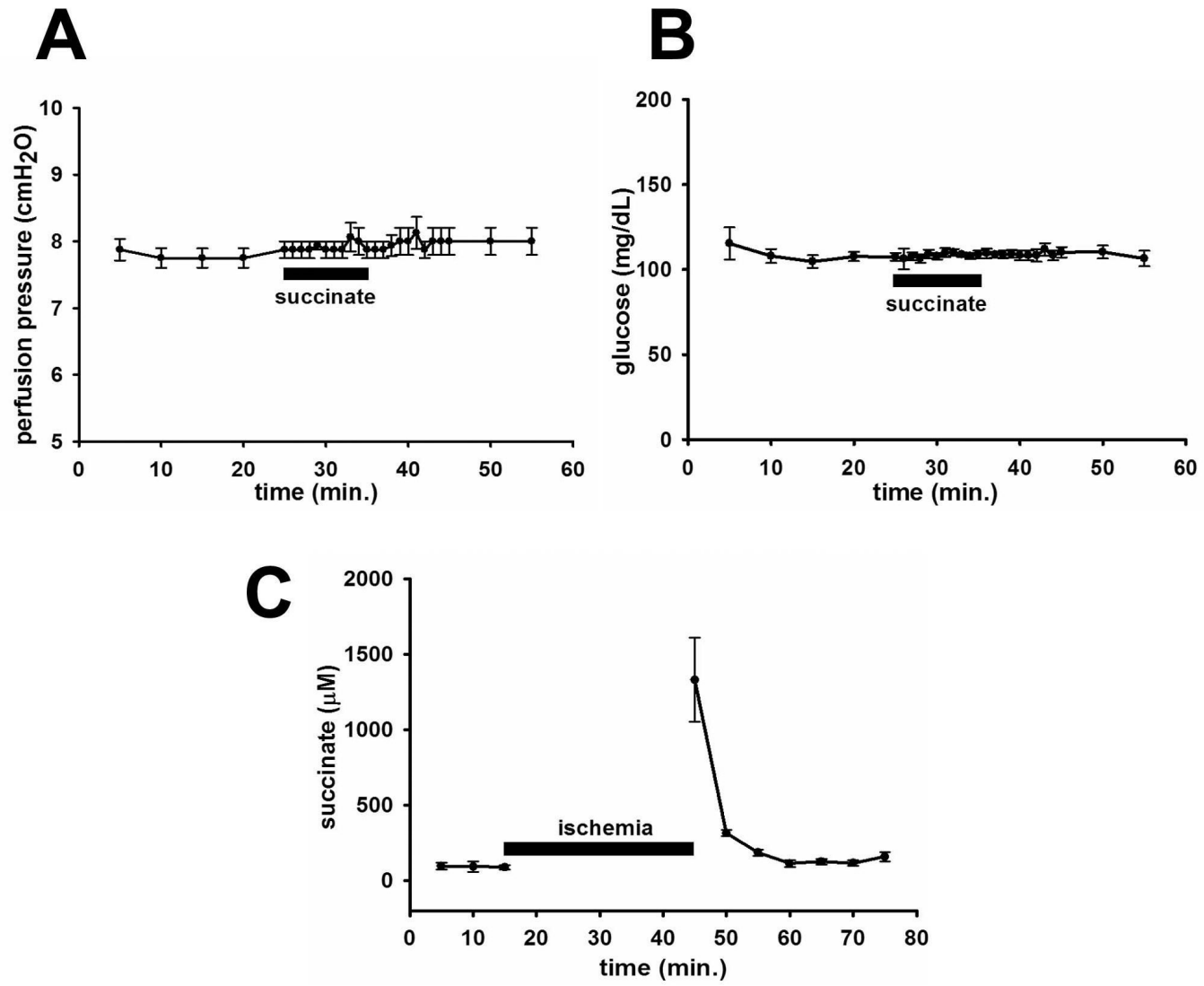

Figure 3.

Succinate in the isolated perfused rat liver. Infusion of succinate (100 μM) into the portal vein does not affect **(a)** perfusion pressure (n=4) or **(b)** glucose output (n=3). Values represent mean ±SEM. **(c)** Succinate levels in perfusate outflow rise 14-fold after ischemia (n=3). Values represent mean±SD.

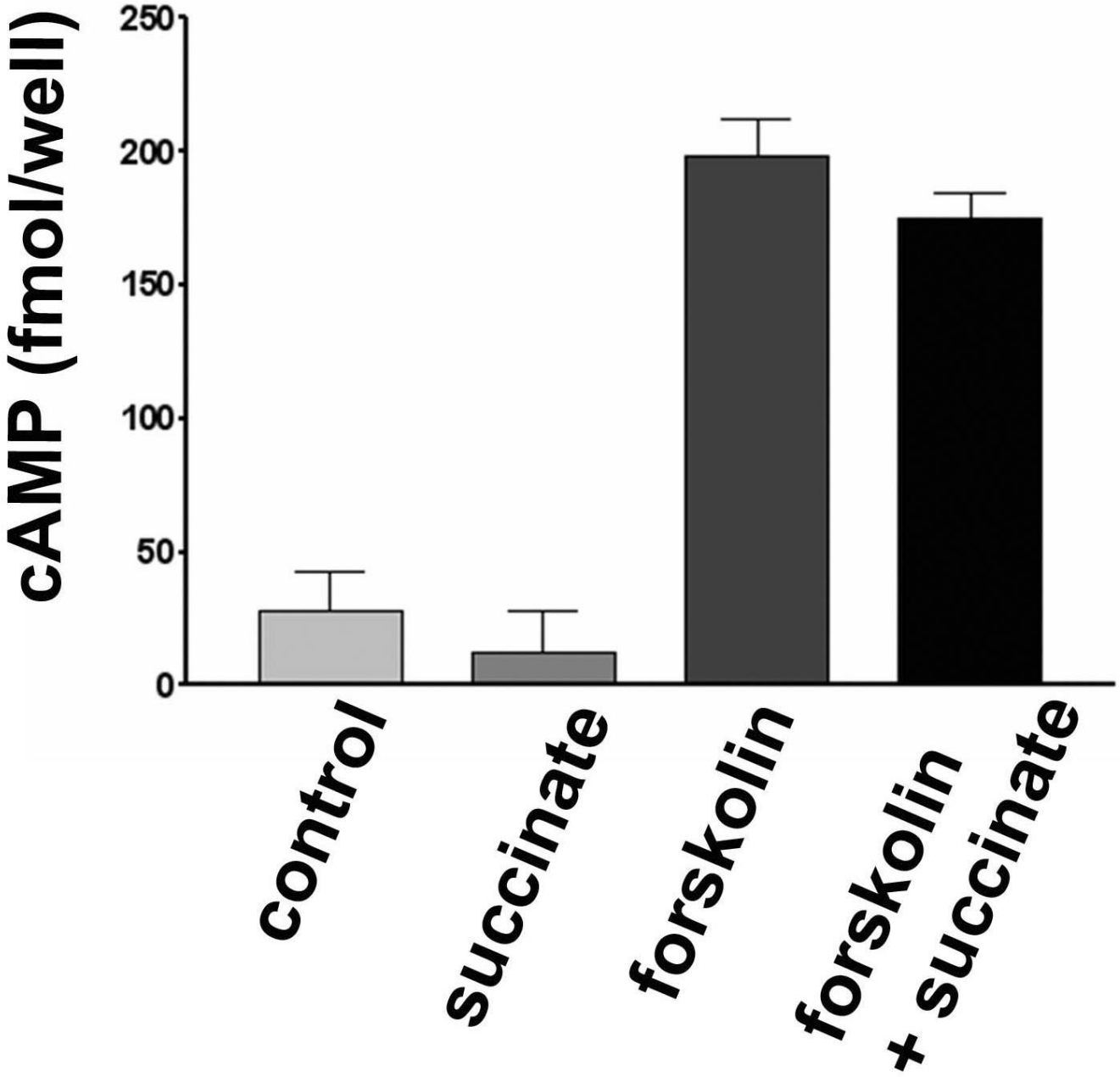

Figure 4.

Succinate does not inhibit the production of cAMP induced by forskolin in quiescent hepatic stellate cells. Bar graph representing cAMP production in non-stimulated (control) stellate cells and in cells treated with succinate (1 mM), forskolin (10 μM) and forskolin plus succinate. Values represent mean±SD of quadruplicate measurements.

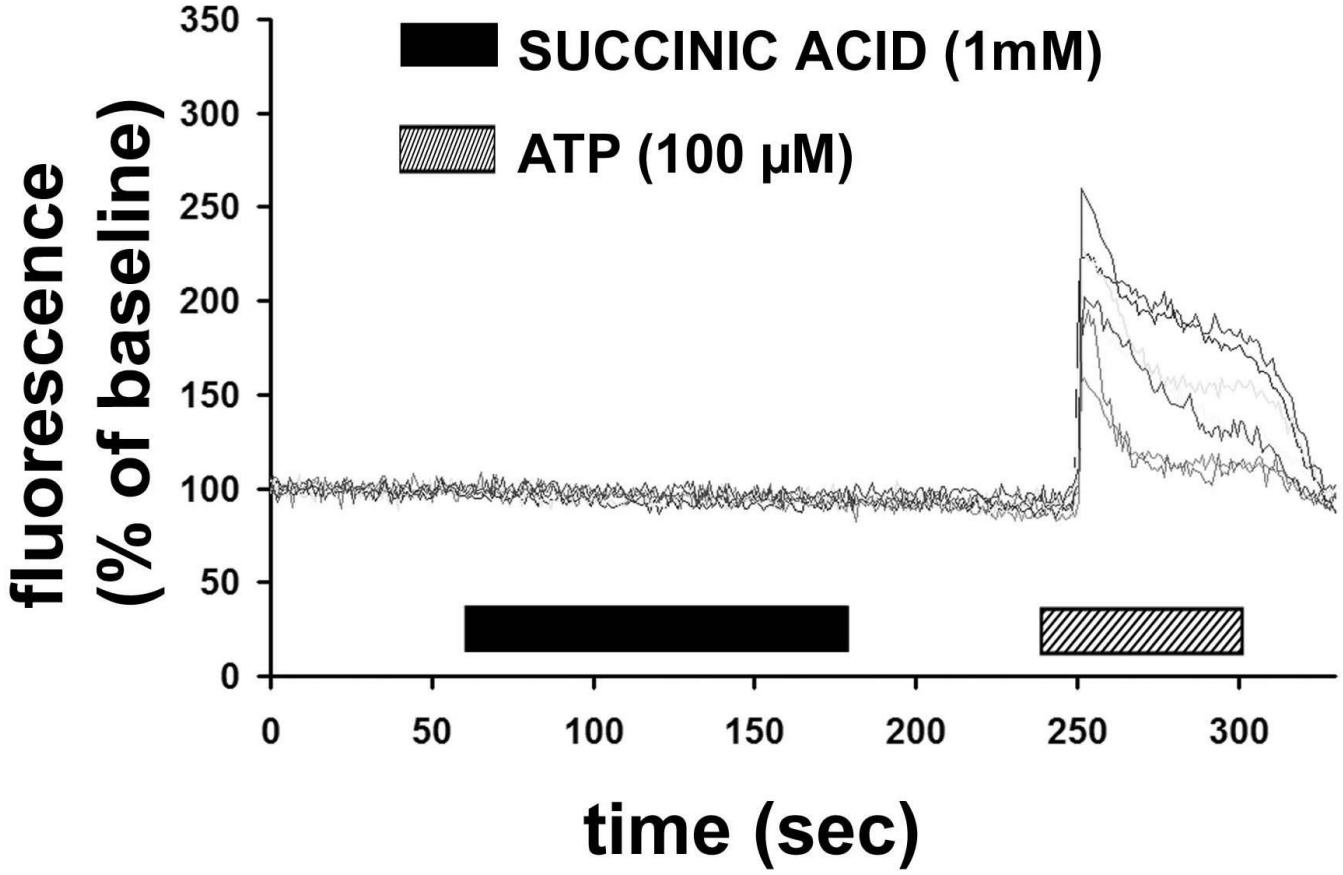

Figure 5.

Succinate does not increase cytosolic Ca^{2+} in hepatic stellate cells. Graphic shows representative tracings of 7 separate quiescent stellate cells serially stimulated with succinate (1 mM), and then the positive control ATP (100 μM). Cells were loaded with the fluorescent Ca^{2+} dye Fluo-4/AM, and then monitored using time-lapse confocal microscopy. Increases in free cytosolic Ca^{2+} were measured and are represented as increases in fluorescence intensity relative to baseline. Results are representative of what was observed in 132 separate stellate cells from 3 separate preparations.

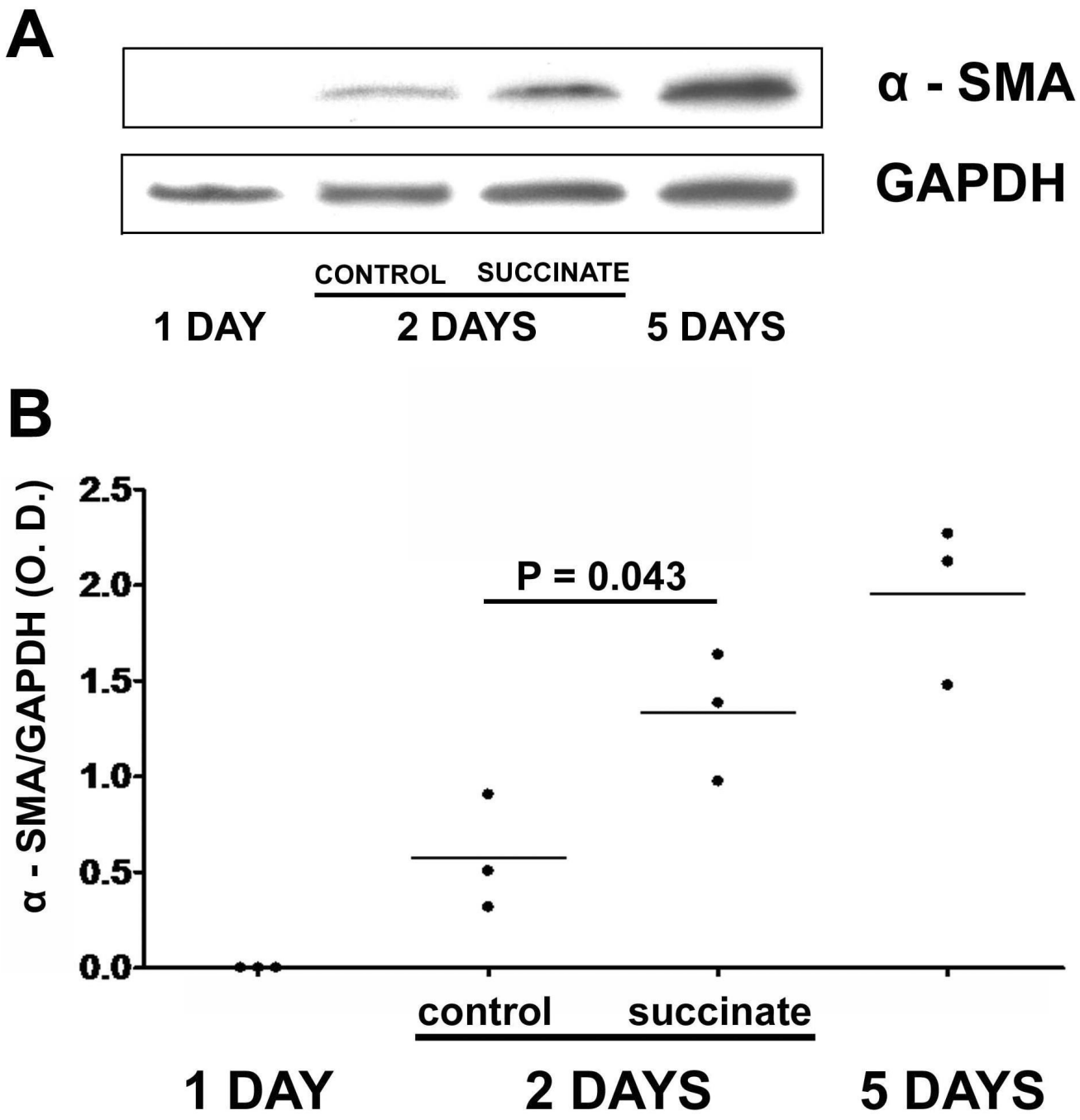

Figure 6.

Succinate promotes activation of hepatic stellate cells. **(a)** Western blot for alpha-smooth muscle actin (α-SMA) in hepatic stellate cells 1, 3, and 5 days after isolation. Three-day HSC were followed either in the absence or presence of succinate (400 μM). **(b)** Densitometric quantification of western blots for α-SMA, normalized by GAPDH expression. Results of each of three separate experiments at each time point are shown. α-SMA expression is increased 2.3-fold in succinate-treated cells relative to untreated controls ($p<0.05$).